Atmospheric Environment 71 (2013) 245–250

Contents lists available at SciVerse ScienceDirect

Atmospheric Environment

journal homepage: www.elsevier.com/locate/atmosenv

Synergistic ammonia losses from animal wastewater

Sang R. Lee [a,*], Scott R. Yates [a], Wayne P. Robarge [b], Scott A. Bradford [a]

[a] USDA-ARS United States Salinity Laboratory, 450 West Big Springs Road, Riverside, CA 92507, United States
[b] Department of Soil Science, North Carolina State University, Raleigh, NC 27695, United States

HIGHLIGHTS

- Measured ammonia emissions from pure $(NH_4)_2SO_4$ solution and animal wastewater.
- Observed enhanced ammonia emissions from both swine and dairy wastewater.
- Multiple reactions in animal wastewater control NH_3 emissions across thin layers.
- Modeling application needs to go with better understanding of ammonia emissions.

ARTICLE INFO

Article history:
Received 17 October 2012
Received in revised form
16 January 2013
Accepted 24 January 2013

Keywords:
Ammonia
Carbon dioxide
Bicarbonate
Emissions
Thin-layer model
Swine lagoon
Dairy waste
Henry's law constant

ABSTRACT

Thin-layer models are commonly used to estimate NH_3 emissions from liquid waste. However, such models differ in their ability to accurately reproduce observed emissions, which may be partly due to an incomplete mechanistic understanding of NH_3 volatilization. In this study, NH_3 release from pure solutions of $(NH_4)_2SO_4$ (AS), swine pit liquid (PL), swine lagoon liquid (LL), dairy lagoon liquid (DLL), and dairy manure liquid (DML) were evaluated under controlled conditions (pH 7.6 and temperature 20 °C). Relationships between the NH_3 release and pH, temperature, and total ammoniacal nitrogen (TAN) were established. Under similar TAN conditions, the NH_3 release was higher for PL, LL, DLL, and DML than for AS. Pure solutions of AS that were spiked with $NaHCO_3$ showed NH_3 emissions rates that were comparable to DML, DLL, LL and PL. The enhanced NH_3 emissions of PL, LL, DLL and DML were therefore explained by linkages between TAN and HCO_3^-.

Published by Elsevier Ltd.

1. Introduction

Animal feed operations (AFOs) are estimated to account for 71% of the total human-induced NH_3 emissions in the United States (USEPA, 2004). Atmospheric deposition of NH_3 can contribute to eutrophication of surface waters (Paerl, 1995), over-fertilization of crops (Galloway and Dentener, 2004), and soil acidification (Van Breemen et al., 1982). Furthermore, NH_3 emission from AFOs is regarded as a significant source for atmospheric particular matter <2.5 μm (Qi and Kleeman, 2006), $PM_{2.5}$. Health studies indicate that exposure of individuals to $PM_{2.5}$ is associated with increased risks of respiratory and cardiovascular problems (Franklin and Zeka, 2006). In addition, $PM_{2.5}$ levels influence haze formation (Trijonis et al., 1991). An understanding of factors that influence NH_3 emission from AFOs is therefore essential for ecosystem and human health.

In dilute solutions, the equilibrium partitioning of NH_3 between the liquid and gas phases is described using Henry's Law (Sawyer and McCarty, 1978; Buonicore and Davis, 1992; Stumm and Morgan, 1995):

$$v_p = k_H C \quad (1)$$

where v_p is the vapor pressure of the gaseous species, C is the concentration of the dissolved gaseous species in the liquid phase, and k_H is the Henry's Law constant. Eq. (1) implies that the emission of NH_3 from a liquid phase would be controlled by the concentration of dissolved NH_3 within the liquid phase (Sawyer and McCarty, 1978; Buonicore and Davis, 1992; Stumm and Morgan, 1995), which in turn depends on the concentration of ammonium (NH_4^+) in solution as demonstrated in the following mass law expression:

* Corresponding author.
E-mail addresses: soilsang@gmail.com, Sang.Lee@ars.usda.gov5 (S.R. Lee).

1352-2310/$ – see front matter Published by Elsevier Ltd.
http://dx.doi.org/10.1016/j.atmosenv.2013.01.046

$$NH_4^+ + OH^{-1} = NH_{3(aq)} + H_2O \quad (2)$$

where $_{(aq)}$ means as a dissolved gas in solution. Eq. (2) illustrates that the concentration of dissolved NH_3 is a direct function of the concentration of NH_4^+ in solution and pH. Under conditions of constant pH, increasing the concentration of NH_4^+ in solution should increase NH_3 emissions due to the corresponding increase in dissolved NH_3 concentrations in the liquid phase. In theory, there is no upper limit on the possible NH_3 emissions with increasing NH_4^+ concentrations in solution.

Wastewaters from AFOs are complex multicomponent chemical mixtures that contain bacteria. Some researchers have found that NH_3 emission is dependent on the solution chemistry condition (Berger and Libby, 1969; Ni et al., 2009). Furthermore, microbial activity in the wastewater is expected to influence many of these reactions. NH_3 emissions from wastewaters are therefore likely to be much more complicated than Eq. (2) suggests. For example, microbially mediated production of CO_2 and/or production and consumption of other gases (e.g., volatile organic carbons) may influence the emission of NH_3 (Chai et al., 2005). Ni et al. (2009) developed a model that includes a dependency of NH_3 emission on CO_2. The emission of NH_3 is also well-known to be dependent on temperature (Loeher, 1984; Jayaweera and Mikkelsen, 1990) which influences the rates of chemical reactions and microbial activity, as well as diffusion coefficients. For example, the value of k_H is a function of temperature that can be described using the Arrhenius equation (Stumm and Morgan, 1995).

Thin-film mass transfer models are commonly used to estimate NH_3 emissions from liquid animal wastes (Ni et al., 2000). The underlying assumption of this approach is that the mass transfer rate of a gas compound from a liquid to the overlying air is controlled by the rates of diffusion through the boundary layers on each side of the interface. When the liquid phase is well mixed, the diffusive NH_3 flux (J_{gw}) is commonly described using a quasi-steady approximation of Fick's first law for diffusion in the gas phase as:

$$J_{gw} = K_{gw}(k_H C - C_g) \quad (3)$$

where K_{gw} is the mass transfer coefficient and C_g and C, respectively, are the bulk gas phase and liquid phase concentrations of NH_3. The mass transfer coefficient is a function of the diffusion coefficient and the boundary layer thickness. Another central parameter in this modeling framework is the concentration gradient across the boundary layer that depends on the equilibrium concentration ($k_H C$) at the air–water interface (Jury et al., 1991).

Our knowledge about factors that influence NH_3 emissions from wastewaters is currently limited. Empirical and mechanistic models of NH_3 emissions often yield different results, underscoring the need to examine the processes driving emissions (Harper and Sharpe, 1998; Aneja et al., 1997; 1996a, 1996b). An incomplete mechanistic understanding of NH_3 production and emission from wastewater may partly be responsible for this disagreement. The uncertainties surrounding the form and assumptions underlying the thin-film modeling approach are the primary motivation for this study. In this study, NH_3 emissions from pure solutions of $(NH_4)_2SO_4$ (AS), swine and dairy wastewaters were evaluated under controlled laboratory conditions. Relationships between NH_3 fluxes and total ammoniacal nitrogen (TAN = NH_3+NH_4^+), pH, and temperature were examined. Comparison of these relationships across treatments established an experimental framework by which the assumptions underlying the typical thin-film NH_3 emission model were investigated.

2. Methods

2.1. Test solutions

Pure ammonium sulfate (AS) solutions at varying TAN concentrations were prepared using reagent grade AS. Samples of swine liquid waste, lagoon liquid (LL) and pit liquid (PL) were obtained from an anaerobic lagoon and shallow pits under the housing units from a swine finisher facility in Warsaw, NC. The samples of liquid waste from the shallow pits under the housing units at the finisher farm were composites and included liquid from several houses. Dairy wastewater samples were obtained from a trench containing dairy manure and liquid (DML) wastewater, and from a dairy anaerobic lagoon liquid (DLL) wastewater on a dairy farm in San Jacinto, CA. Wastewater samples were placed in 20 L carboys, transported back to the laboratory, and stored at 4 °C until use.

The pH buffer solutions were prepared using nearly equal volumes of 0.1 M KH_2PO_4 solutions and 0.1 M NaOH solution to achieve the desired pH (pH 7.6). The TAN concentration and pH of the DML, DLL, LL and PL samples was controlled by diluting with deionized water, AS solutions, and pH buffer solutions. The final pH of the buffer solutions and the test solutions was determined before and after experiments using a pH meter and combination glass electrode calibrated with NIST-traceable pH standards (Denver UB-10 pH mV^{-1} meter equipped with a High performance pH ATC^{-1} Glass-body Electrode).

The TAN concentration of the AS, PL and LL samples was determined using a steam distillation method (U.S. EPA Method 350.2) that is well documented in the literature (Bremner, 1965; Bundy and Bremner, 1973; Stevenson, 1982a, b). TAN concentration of the AS, DML and DLL samples was determined using an Alpkem/OI Analytical Flow Solution IV with autosampler (U.S. EPA Method 350.1). The Alpkem Flow Solution IV with autosampler was equipped with ammonia/TKN cartridges allowing for a variety of measurements of different forms of nitrogen in solution. Additional details about these analytical methods and quality assurance and control protocols are available in the Supporting information (si).

2.2. Experimental setups

Fig. 1 presents illustrations of two experimental setups that were used to contain test solutions and to measure the emission of NH_3 in response to changes in solution composition, pH, and temperature. The first setup consisted of a 4 L pyrex reagent bottle chamber (RBC) (Fig. 1). The RBC has an internal volume of 4 L (depth 21 cm × diameter 16 cm) and a surface area (S_A) of 201 cm^2 at the air–liquid interface. The inlet (0.8 cm internal diameter) and outlet (0.4 cm internal diameter) of the RBC consisted of valves placed in the interior of a #8 stopper. The RBC was filled with 2 L of a selected test solution and positioned into a water bath. The temperature of the water bath was controlled by an internal heating and refrigeration unit (Forma Scientific CH/P temperature control system). A pump (Cole Parmer Instruments Model Number 7553-00) was used to slowly circulate the test solution in the RBC. The pump rate was set to completely circulate all ~2 L of the test solution once every 20 min. The temperature of the test solution in the RBC was monitored manually at the center location using a digital thermometer with a tolerance of +/− 0.1 °C (Fisher Scientific digi-thermo thermocouples with external stainless steel probes).

To test the validity of results from the RBC to larger scales a second experimental setup was employed. This setup (Fig. 1b) consisted of a simple flow-through teflon-lined chamber (SFTC). The SFTC has a volume of 9 L (length 30 cm × width 20 cm × height 15 cm) and a S_A of 600 cm^2 at the air–liquid interface. Two inlets (~1 cm internal diameter) were used to allow air flow into the

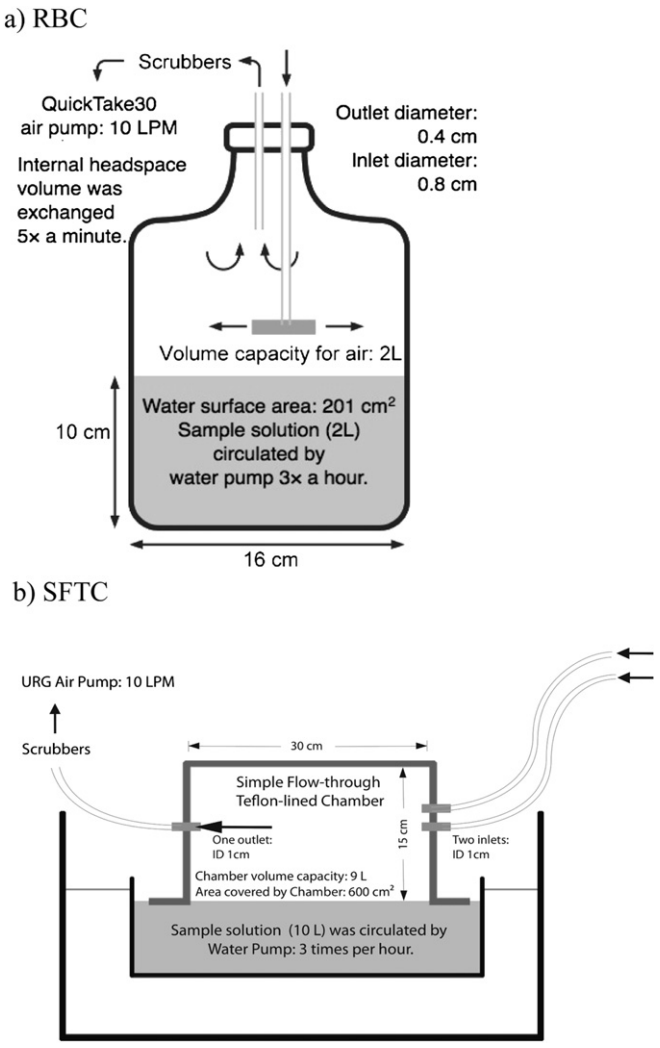

Fig. 1. Schematics of a) reagent bottle chamber (RBC) and b) simple flow-through teflon-lined chamber (SFTC).

chamber. A single outlet (~1 cm internal diameter) was located on the opposite wall of the SFTC. The inlets and outlets were bulkhead fittings which contained internal valves that were only open when the appropriate hose connector was inserted into the fitting. The SFTC was positioned over the test solutions contained in a plastic pan and lowered into the pan until the SFTC was floating on the test solution supported by the flange around the outside of the chamber. Direct contact of the chamber with the test solutions resulted in an air-tight seal of the chamber at the air–liquid interface.

Air flow (Q_a) through the RBC and SFTC setups was held constant at 10 LPM using calibrated air pumps located downstream of the chamber outlet. This translates to effective wind speeds (Q_a/S_A) of approximately 0.008 to 0.003 m s^{-1} in the RBC and SFTC setups, respectively, and limited the impact of turbulence on emissions. NH_3 emitted from the test solutions was scrubbed from the air exiting the chambers using glass scrubbers containing H_2SO_4 solution (0.05 or 0.025 N) and fritted glass on the inlets. Ammonia loss measurements from the test solutions were typically conducted over periods of 1 h after the solution achieved the desired temperature. Additional details about the quality assurance and control protocols are available in the Supporting information.

The design and effective wind speeds of the RBC and SFTC setups were selected to maximize J_{gw}. Eq. (3) indicates that a maximum value of $J_{gw} = K_{gw}k_HC$ occurs when $C_g \approx 0$. Under these conditions the effects of solution chemistry on equilibrium partitioning (k_HC) at the air–liquid interface can be readily examined. Low values of C_g were achieved in RBC and SFTC setups because of short air phase residence times of 0.2 and 0.9 min, respectively. The equilibrium value for $C_g = k_HC/(RT_k)$ was calculated to be around 1688 mg NH_3–N m^{-3} when TAN = 2500 mg NH_4–N m^{-3}; where R is the gas constant and T_k is the temperature in degrees Kelvin. Experimental results presented below were several orders of magnitude lower than this equilibrium prediction. Most of the RBC and SFTC experiments were replicated and some were run in triplicate.

3. Results and discussion

3.1. Performance of the experimental chambers

The performance of the RBC and SFTC setups were assessed by measuring the flux of NH_3 from pure AS solutions under differing TAN concentrations (100–500 mg NH_4–N L^{-1}). Period average measurements of ambient NH_3 concentrations (during ~1 h duration) were obtained by dividing the total mass of NH_3 emitted from the chamber by the total air volume passed through the acid scrubbers. The final calculated ammonia concentration values were standardized to units of mg NH_3–N m^{-3}. Fig. 2 presents a plot of the period average NH_3 concentration as a function of the TAN concentration in pure AS solutions under constant temperature (20 °C) and pH (pH = 7.6) conditions. As predicted by Eq. (2), the measured NH_3 concentration increases linearly with an increase in TAN concentration of the AS solutions. The RBC and SFTC setups gave nearly identical results, demonstrating that findings from the smaller RBC were comparable with the larger SFTC. The corresponding linear regression equations are presented in the figure. At concentrations of TAN > 500 mg NH_4–N L^{-1} there appears to be a definite linear relationship between the calculated NH_3 concentration and TAN. Failure of the regression equations to have a zero intercept is probably due to experimental error in the measurement of low NH_3 concentrations at low TAN. Error bars derived from replicate experiments were very small (Fig. 2). For simplicity, subsequent figures do not include error bars.

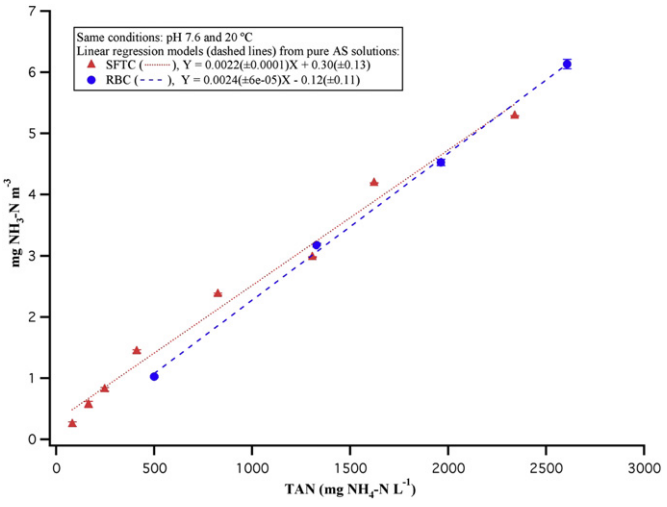

Fig. 2. Measurements of atmospheric NH_3 release from ammonium sulfate (AS) solutions as a function of TAN (pH 7.6, T = 20 °C, SFTC and RBC). Dashed line represents linear regression model (X = TAN, Y = Air Concentration). Error bars on data points were derived from replicate experiments.

3.2. Emissions of NH_3 from AS solutions as a function of pH and temperature

Eq. (2) suggests a dependency of NH_3 emission on pH and temperature (reaction rates and diffusion coefficients are dependent on temperature). Fig. 3 presents the period averaged NH_3 concentration emitted from pure AS solutions in the RBC system at different pH (7.0–8.0) and temperature (10–25 °C) conditions. The TAN concentration of the AS solutions equaled 370 and 412 mg NH_4–N L^{-1} for temperature and pH experiments, respectively. Manual measurements of temperature during these experiments showed temperature control of the test solutions within +/− 0.1 °C. Measurements of pH and TAN concentration before and after the measurement period showed little to no change, demonstrating that the volume of the test solution used and the duration of the test period resulted in no chemical changes. The NH_3 loss from the AS solution increases exponentially with water temperature and pH (Fig. 3). These observations are consistent with expectations based on Eq. (2) and the Arrhenius equation (Stumm and Morgan, 1995).

3.3. Emissions of NH_3 from animal wastewater

Fig. 4 presents plots of the period averaged NH_3 concentrations from AS and AFO wastewaters (PL, LL, DML and DLL) at constant temperature (20 °C) and pH (pH = 7.6) as a function of TAN. Typically, the TAN of the DML and PL samples was higher than the DLL and LL samples. The extended TAN concentrations for the PL, LL, DML and DLL samples were obtained by spiking with solid reagent-grade AS. The response in the emitted NH_3 concentration with changes in TAN of the wastewaters was linear over the range of tested TAN. This result indicates that spiking the wastewaters with AS was a valid approach. Regression equations for the emitted NH_3 concentration and the TAN concentration are also presented in the figure. The calculated uncertainty associated with the intercept values was consistent with zero NH_3 emissions as TAN approaches zero.

Although the response in the emitted NH_3 concentration with TAN was linear for the PL, LL, and DML wastewater solutions, the absolute magnitude of the calculated NH_3 concentration differed

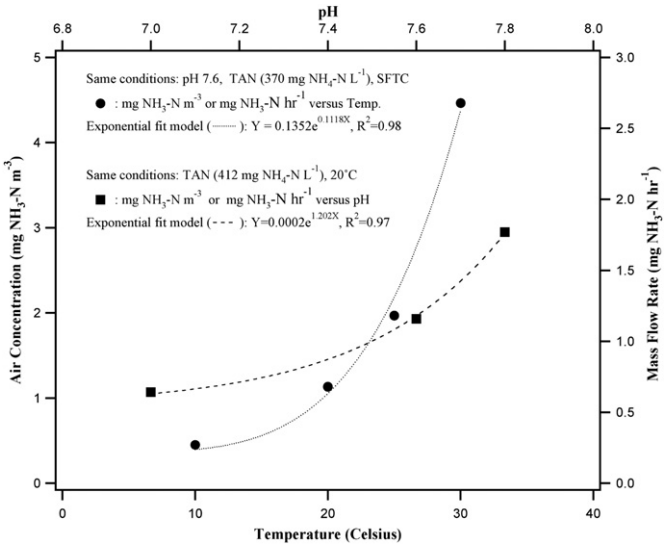

Fig. 3. Measurements of atmospheric NH_3 release from pure ammonium sulfate (AS) solutions as a function of temperature (TAN 370 mg NH_4–N L^{-1}, pH 7.6) and pH (TAN 410 mg NH_4–N L^{-1}, T = 20 °C) using SFTC. Dashed lines represent linear regression models.

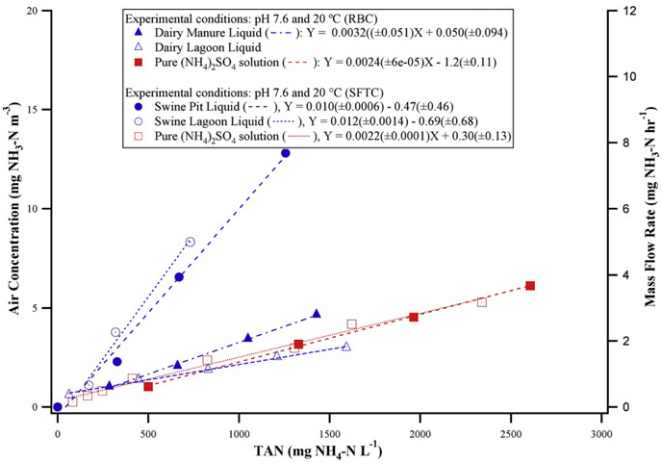

Fig. 4. Comparison of the measured atmospheric NH_3 release from pure $(NH_4)_2SO_4$ solutions, swine pit liquid (PL), swine lagoon liquid (LL) solutions, dairy manure liquid (DML) solutions, and dairy lagoon liquids (DLL) solutions. Dashed lines represent the respective linear regression models. Original TAN content for DLL was <126 mg NH_4–N L^{-1} and for DML was <570 mg NH_4–N L^{-1}.

significantly from that observed with the pure AS solutions. The emitted NH_3 concentration from the swine wastewater sample solutions was ~5 times higher than the values from pure AS solutions. Similarly, the emitted NH_3 concentration from the DML sample was ~1.4 times higher than the value from pure AS solutions.

In contrast to DML, DLL samples only demonstrated a slight enhancement in NH_3 concentrations compared to the pure AS solutions by ~900 mg NH_4–N L^{-1}. Spiking DLL with solid AS in excess of 900 mg NH_4–N L^{-1} actually resulted in a suppression of the NH_3 emissions. The linearity of NH_3 concentrations from the DML and DLL samples was investigated at higher TAN concentrations. At higher TAN, the increase in NH_3 concentrations from DLL appears to once again to become linear with an increase in the TAN. The difference in the absolute magnitude of NH_3 concentrations for DML and DLL samples at the higher TAN concentrations were directly related to the original TAN concentration in the wastewater samples. Hence, differences in NH_3 release behavior of DML and DLL samples were attributed to the original TAN content of these samples; e.g., the TAN was relatively low (<126 mg NH_4–N L^{-1}) for DLL compared to that of DML (<570 mg NH_4–N L^{-1}).

A primary focus of this study is to better quantify the contributing reactions that enhance NH_3 emissions from animal wastewater compared to AS. Results summarized in Fig. 4 suggest that, in general, wastewaters have greater NH_3 emissions. This suggests that other reactions and processes are influencing NH_3 emissions and release in wastewater systems. Similar to AS solutions (see Fig. 2), Eq. (2) appears to be the dominant reaction driving NH_3 emissions in the wastewater at higher TAN concentrations, without any corresponding increase of other constituents in the liquid waste. When compared with AS solutions at similar TAN levels, the enhanced emission of NH_3 in wastewaters indicates that at additional reactions are contributing to the higher NH_3 emissions.

3.4. Impact of $NaHCO_3$ on NH_3 emissions

The challenge is to determine why compositional differences in wastewater and pure AS solutions could lead to differences in $NH_{3(aq)}$ concentration near the air–liquid interface. This requires that other reactions are occurring in solution and contributing to dissolved $NH_{3(aq)}$ beyond the basic relationship between NH_4^+ and dissolved $NH_{3(aq)}$ given in Eq. (2). Animal wastewaters are complex

mixtures containing relatively high concentrations of bacteria, dissolved organic compounds, salts, and various fats and oils excreted by the animals or from feed spillage. These wastes also emit H_2S, CO_2 and VOCs as well as NH_3 across the air–liquid interface. In particular, elevated levels of dissolved CO_2 could be present in wastewater due to microbial respiration, and CO_2 is expected to play a role in a variety of biogeochemical reactions. Hence, contributing reactions to NH_3 emission could be dependent on dissolved sulfide, carbonate and organic acid. A series of screening tests was therefore conducted to determine whether various agents (surfactant, organic acid, methanol, and sodium bicarbonate) could promote or depress NH_3 emissions from either the pure AS solutions or wastewater. Of the agents used in the screening trials, only bicarbonate produced a response in emissions similar to that observed for PL, LL, DML and DLL (Table S1 in the SI).

Additional RBC experiments were therefore conducted to test whether CO_2 could promote NH_3 emissions from pure AS solutions and animal wastewaters at constant pH (pH = 7.6) and temperature (T = 20 °C), and if a quantitative response could be determined. Sodium bicarbonate was added to simulate the potential influence of elevated partial pressure of CO_2 on emissions. Bicarbonate anion is the dominant form of dissolved carbonate species in solution at pH = 7.6 (Stumm and Morgan, 1995). Results for spiking $NaHCO_3$ into AS solutions and animal wastewaters at different TAN are presented in Figs. 5 and 6, respectively. Regression equations are summarized in Table S2 in the SI. Enhanced NH_3 emissions were observed in Fig. 5 from AS solutions at the same TAN concentration when spiked with bicarbonate (0.036, 0.056, 0.084 M) (Table S3 in the SI). When these results are plotted as a function of HCO_3^-/NH_4^+ molar ratio, the observed response showed ~2 times higher NH_3 emissions than the AS solutions without HCO_3^-. The rate of increase in NH_3 emissions (derivative of the curve) was higher at lower values of HCO_3^-/NH_4^+ and then decreased at higher TAN. Similarly, addition of HCO_3^- to the animal wastewaters yielded an initial enhancement in the NH_3 emissions that decreased with increasing TAN (Fig. 6). This would explain why the derivative of the curve in NH_3 emissions at higher TAN concentrations in the animal wastewater approaches that observed for the pure AS solutions.

These observations suggest that the enhancement mechanism/reaction of NH_3 emissions is strictly related to the presence of bicarbonate. In other words, despite the complexity of animal

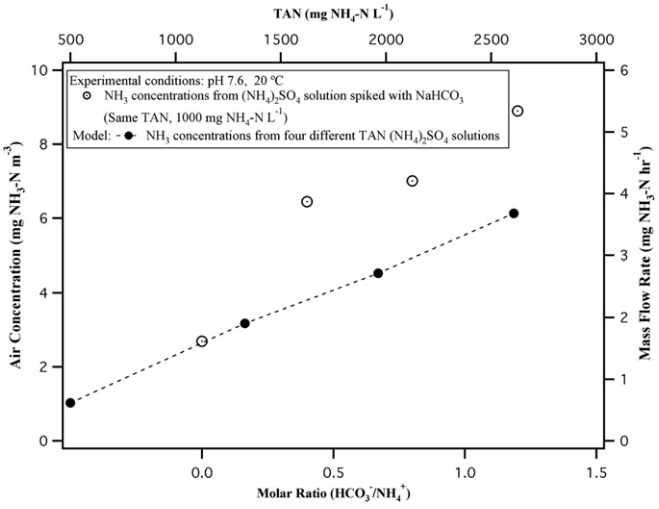

Fig. 5. Measurements of atmospheric NH_3 release from pure ammonium sulfate (AS) solutions. AS solutions spiked with $NaHCO_3$ as a function of TAN (pH = 7.6, T = 20 °C) using RBC. Spiked solutions were generated by adding reagent-grade $NaHCO_3$ (0, 0.4, 0.8, 1.2 molar ratio of HCO_3^-/NH_4^+) to fresh 2 L portions of pure AS solutions of 1000 mg NH_4–N L^{-1} TAN. Dashed lines are added to better visualize trends in NH_3 emissions.

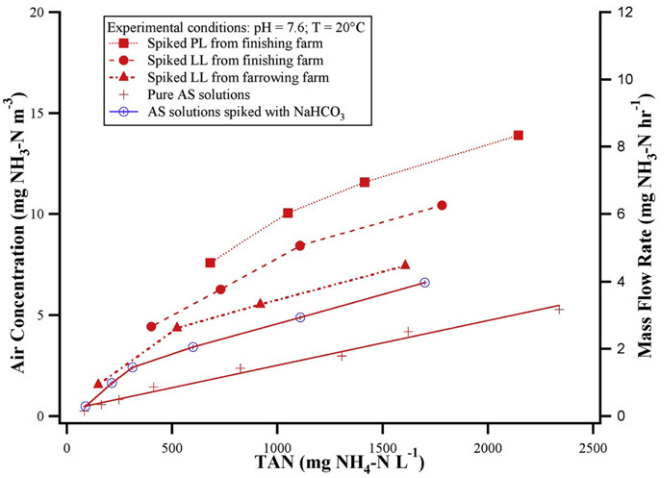

Fig. 6. Comparison of the measured atmospheric NH_3 release between original and spiked test solutions of liquid animal waste and pure AS solutions as a function of increasing TAN (pH = 7.6, T = 20 °C). Spiked solutions were generated by adding reagent-grade ammonium sulfate to fresh 10 L portions of liquid animal waste to obtain desired TAN. Dashed lines and zero TAN points added to better visualize trend in NH_3 emissions. Solid line through AS data represents linear regression model.

wastewater, this enhancement is due to the influence of HCO_3^- either directly or indirectly on the production of $NH_{3(aq)}$, which at lower concentrations of TAN, is more efficient in producing $NH_{3(aq)}$ than Eq. (2). Eq. (2) and the following chemical reactions provide a partial explanation for the observed dependence of NH_3 emission on NH_4^+, pH and HCO_3^- as:

$$NH_4^+ + HCO_3^- = NH_{3(aq)} + H_2CO_{3(aq)} \quad (4)$$

$$H_2CO_{3(aq)} = H^+ + HCO_3^- \quad (5)$$

$$H_2CO_{3(aq)} = H_2O + CO_2 \quad (6)$$

It should be mentioned that other reactions that involve carbonate (CO_3^{2-}) are also possible. However, at pH 7.6 bicarbonate is the dominant carbonate ion (~95%) and dissolved carbonic acid makes up only around 5% of the carbonate ions (Stumm and Morgan, 1995).

Changes in NH_3 flux observed with additions of bicarbonate to the pure AS solutions (Fig. 5) can be explained in part by considering Eqs. (2) and (4)–(6). Similar to Eq. (2), Eq. (4) predicts that $NH_{3(aq)}$ is related to TAN in a linear fashion. However, the decreasing slope in NH_3 emissions with increasing TAN suggests that Eq. (4) may not be solely involved in enhancing the production of $NH_{3(aq)}$, or that Eq. (4) becomes kinetically limited possibly due to transport limitations near the air–liquid interface. For example, loss of CO_2 across the air–liquid interface consumes $H_2CO_{3(aq)}$ and this would tend to enhance NH_3 emissions. The amount of bicarbonate added to the pure AS solutions (equivalent concentration = 0.02 M) was not limiting at the calculated NH_3 fluxes measured with the RBC. Thus with increasing TAN, the destruction of $H_2CO_{3(aq)}$ would become the rate-limiting step effectively maximizing the production of $NH_{3(aq)}$ by Eq. (4). Further production of $NH_{3(aq)}$ would continue via Eq. (2) with an increase in TAN, but at relatively lower amounts of $NH_{3(aq)}$ per unit increase in TAN.

The influence of HCO_3^- on NH_3 emissions from the various wastewaters (Figs. 4 and 6) was even more complicated than in pure AS solutions (Fig. 5). Enhanced emissions from the animal wastewater were related to the initial TAN concentration in the test

solution, with the limit in enhanced NH_3 emissions substantially exceeding that observed in the spiked pure AS solutions, especially for the LL, PL, and DML samples. If the rate of loss of CO_2 across the air–liquid interface (which consumes $H_2CO_{3(aq)}$) was the limiting step, it is not clear why this restriction was present in the pure AS solutions, but not in the LL, PL, DML and DLL solutions at the same TAN concentration. The apparent dependence on the concentration of TAN and the enhanced NH_3 emissions suggests a link between TAN and the enhancement factor in the wastewater. For example, higher TAN in the wastewater could be associated with higher dissolved solids and higher respiration rates of bacteria in solution. Higher production of CO_2 in solution would drive aqueous carbonate chemistry to produce higher concentrations of bicarbonate in solution. However, this would not necessarily increase the production of $NH_{3(aq)}$ if the rate of loss of CO_2 across the air–liquid interface is the rate limiting step. It would therefore appear that a number of factors are influencing the extent of the reaction for Eq. (4) that eventually limits the production of $NH_{3(aq)}$ as a function of TAN in solution. The factors could include the overall energetics of Eq. (4) as well as possible transport of reactive species from the bulk solution to the region near the air–liquid interface. Additional research studies are needed to full resolve these issues.

3.5. Modeling implications

Ammonia emissions increased in a linear fashion with increasing TAN for the pure AS solutions (Fig. 2). This was consistent with the expected results (Eq. (2)) and the assumption that the Henry's Law coefficient is indeed constant over a range of dissolved $NH_{3(aq)}$ in solution. The linearity in NH_3 emissions from spiked animal wastewater (Fig. 3) also suggests that the value of the Henry's Law coefficient remained unchanged. Consequently, it is logical to assume that the enhanced emission of NH_3 from wastewater compared with pure AS solutions (Fig. 4) was due differences in the concentration of dissolved $NH_{3(aq)}$ near the air–liquid interface as a result of HCO_3^-.

4. Conclusions

The results from this study suggest that current models such as thin-film and process-based models being developed to predict NH_3 emissions from AFOs waste liquid system could be in error if it is assumed a single reaction is controlling NH_3 emissions across the air–liquid interface (i.e. Eq. (2)). While any model can be made to fit observed data, failure to account for the apparent complexity in reactions controlling NH_3 emissions from animal wastewater have the potential to generate misleading results when used to test the effects on NH_3 emissions from possible remediation strategies or alternative management practices to handle the waste.

Appendix A. Supplementary data

Supplementary data related to this article can be found at http://dx.doi.org/10.1016/j.atmosenv.2013.01.046.

References

Aneja, V.P., Kim, D.S., Das, M., Hartsell, B.E., 1996a. Measurements and analysis of reactive nitrogen species in the rural troposphere of southeast United States: southern oxidant study site Sonia. Atmospheric Environment 30 (4), 649–659.

Aneja, V.P., Robarge, W.P., Sullivan, L.J., Moore, T.C., Pierce, T.E., Geron, C., Gay, B., 1996b. Seasonal variations of nitric oxide flux from agricultural soils in the southeast United States. Tellus 48 (B), 626–640.

Aneja, V.P., Chauhan, J.P., Walker, J.T., 1997. Characterization of atmospheric ammonia emissions from dairy waste storage and treatment lagoons. Geophysical Research 105 (D9), 11535–11545.

Berger, R., Libby, W.F., 1969. Equilibration of atmospheric carbon dioxide with seawater: possible enzymatic control of the rate. Science 194, 1395–1397.

Bremner, J.M., 1965. Organic forms of nitrogen. In: Methods of Soil Analysis. Agron. Monogr., vol. 9. ASA Edn, Madison, WI, pp. 1238–1255.

Bundy, L.G., Bremner, J.M., 1973. Determination of ammonium n and nitrate n in acid permanganate solution used to absorb ammonia, nitric oxide, and nitrogen dioxide evolved from soils. Communications in Soil Science and Plant Analysis 4 (3), 179–184.

Buonicore, A.J., Davis, W., 1992. Air Pollution Engineering Manual. Air and Waste Management Association, New York, N.Y.

Chai, X.-S., Falabella, J.B., Teja, A.S., 2005. A relative headspace method for Henry's constants of volatile organic compounds. Fluid Phase Equilibria 231 (2), 239–245.

Franklin, M., Zeka, A., 2006. Association between PM2.5 and all-cause and specific-cause mortality in 27 US communities. Journal of Exposure Science & Environmental Epidemiology 17 (3), 279–287.

Galloway, J.N., Dentener, F.J., 2004. Nitrogen cycles: past, present, and future. Biogeochemistry 70 (2), 153–226.

Harper, L.A., Sharpe, R.R., 1998. Ammonia Emissions from Dairy Waste Lagoons in the Southeastern U. S. Coastal Plains, Technical report (Available from:L. A. Harper, USDA-ARS, 1420 Experiment Station Road, Watkinsville, GA 30677).

Jayaweera, G.R., Mikkelsen, D.S., 1990. Ammonia volatilization from flooded soil systems: a computer model: I. Theoretical aspects. Soil Science Society of America Journal 54 (5), 1447–1455.

Jury, W.A., Gardner, W.R., Gardner, W.H., 1991. Soil Physics, fifth ed. John Wiley & Sons.

Loeher, R.C., 1984. Pollution Control for Agriculture, second ed. Academic Press, New York, N.Y.

Ni, J.-Q., Hendriks, J., Vinckier, C., Coenegrachts, J., 2000. A new concept of carbon dioxide accelerated ammonia release from liquid manure in pig house. Environment International 26 (1–2), 97–104.

Ni, J.Q., Heber, A.J., Sutton, A.L., Kelly, D.T., 2009. Mechanisms of gas releases from swine wastes. Transactions of ASABE 52, 2013–2025.

Paerl, H.W., 1995. Coastal eutrophication in relation to atmospheric nitrogen deposition: current perspectives. Ophelia 41, 237–259.

Qi, Ying, Kleeman, M.J., 2006. Regional source contribution to secondary particulate matter in California using a three-dimensional source-oriented air quality model. Atmospheric Environment 40 (3), 736–752.

Sawyer, C.N., McCarty, P.L., 1978. Chemistry for Environmental Engineering, third ed. McGraw-Hill, New York, N.Y.

Stevenson, F.J., 1982a. Nitrogen-organic forms. In: Methods of Soil Analysis. 2nd Agron. Monogr, vol. 9. ASA and SSSA Edn, Madison, WI, pp. 625–641.

Stevenson, F.J., 1982b. Nitrogen-organic forms. In: Methods of Soil Analysis, SSSA Book Ser. 5. Agron. Monogr., vol. 9. SSSA Edn, WI.Madison, pp. 1185–1200.

Stumm, W., Morgan, J.J., 1995. Aquatic Chemistry: Chemical Equilibria and Rates in Natural Waters, third ed. John Wiley & Sons, Inc, 605 Third Avenue, New York, NY.

Trijonis, J.C., Malm, W.C., Pitchford, M., White, W.H., 1991. Visibility: existing and historical conditions – causes and effects. In: Irving, P.M. (Ed.), Acidic Deposition: State of Science and Technology. Terrestrial, Materials, Health and Visibility Effects, vol. III. The US National Precipitation Assessment Program, Washington, D. C (State of Science and Technology Report no.24).

USEPA (US Environmental Protection Agency), 2004. Estimating ammonia emissions from anthropogenic nonagricultural sources – draft final report. In: Emission Inventory Improvement Program. US Environmental Protection Agency, Washington, DC. http://www.epa.gov/ttnchie1/eiip/techreport/volume03/eiip_areasourcesnh3.pdf.

Van Breemen, N., Burrough, P.A., Velthorst, E.J., Van Dobben, H.F., Wit, T. de, Ridder, T.B., Reijnders, H.F.R., 1982. Soil acidification from atmospheric ammonium sulphate in forest canopy throughfall. Nature 299, 548–550.